

**Supplementary Information for:**

**The heterogeneity of oxidized lipids in individual tumor cells reveals  
NK cell-mediated cytotoxicity by label-free mass cytometry**

Zizheng Shen,<sup>a</sup> Huan Yao,<sup>ab</sup> Jinlei Yang,<sup>a</sup> Xingyu Pan,<sup>a</sup> Hansen Zhao,<sup>a</sup> Guojun  
Han,<sup>cde</sup> Sichun Zhang,<sup>\*a</sup> and Xinrong Zhang<sup>a</sup>

<sup>a</sup> Department of Chemistry, Tsinghua University, Beijing 100084, P.R. China.

<sup>b</sup> Division of Chemistry and Analytical Science, National Institute of Metrology,  
Beijing 100029, P.R. China.

<sup>c</sup> Institute of Medical Technology, Peking University Health Science Center, Beijing,  
100191, P.R. China.

<sup>d</sup> Peking University School and Hospital of Stomatology, Beijing, 100081, P.R.  
China.

<sup>e</sup> Department of Biomedical Engineering, Peking University Health Science Center,  
Beijing, 100191, P.R. China.

\*Prof. Sichun Zhang: [sczhang@mail.tsinghua.edu.cn](mailto:sczhang@mail.tsinghua.edu.cn)

## Table of Contents

<b>Figure S1.</b> The detection of lipids in individual HepG2 cells. ....	3
<b>Figure S2.</b> The heat map of individual HepG2 cells co-cultured with different amount of NK92 MI cells from E:T 0:1(control group) to 10:1. ....	4
<b>Figure S3.</b> The scatter plot of individual HepG2 cells co-cultured with different amount of NK92 MI cells from E:T 1:1 to 10:1. ....	5
<b>Figure S4.</b> The logarithmic radar charts of average relative intensities of 69 lipids and oxidized lipids. ....	6
<b>Figure S5.</b> The relative intensities of different lipids between control group and NK group. ....	7
<b>Figure S6.</b> The changes of oxidized lipids in individual HepG2 cells after co-culturing with NK cells. ....	8
<b>Figure S7.</b> The MS <sup>2</sup> of PC(38:6), PC(38:6-2OH), PC(34:2) and PC(34:2-2OH). ....	9
<b>Figure S8.</b> The changes of ROS and Fe <sup>2+</sup> in NK group and erastin group. ....	10
<b>Figure S9.</b> The heat map of individual HepG2 cells with and without incubating with erastin. ....	11
<b>Table S1.</b> 69 lipids annotated by accurate <i>m/z</i> . ....	12

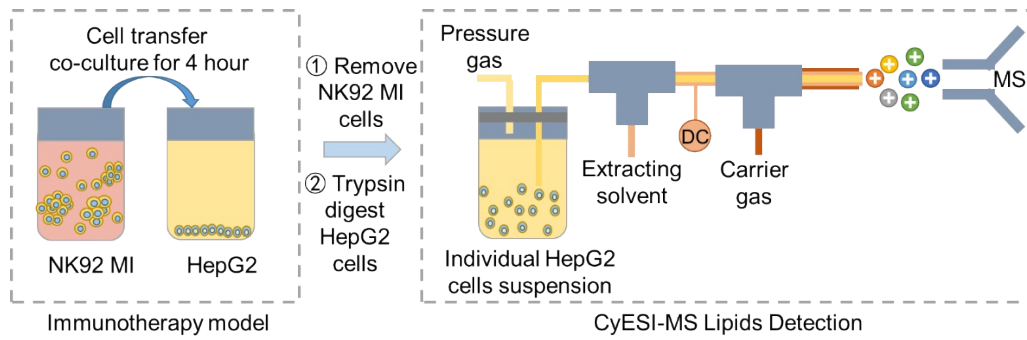


**Figure S1.** The detection of lipids in individual HepG2 cells.

The NK cell-mediated apoptosis model was established by co-culturing HepG2 cells with NK92 MI cells for 4 hours. After removing NK92 MI cells and digesting HepG2 cells with trypsin, the individual HepG2 cells suspension was obtained. The individual HepG2 cells were pumped into the self-made CyESI system by pressure gas. Lipids information were obtained simultaneously by mass spectrometry.

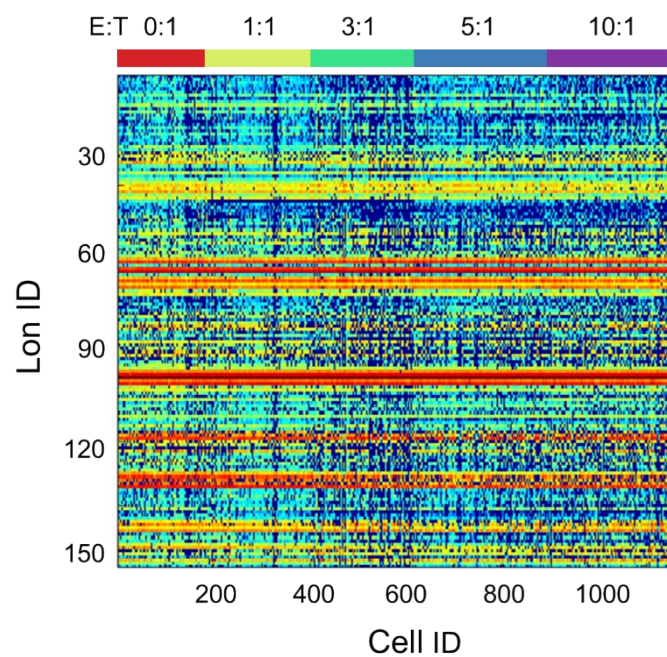


**Figure S2.** The heat map of individual HepG2 cells co-cultured with different amount of NK92 MI cells from E:T 0:1(control group) to 10:1.

Each column of the heat map represented an individual cell and each row represented a cell-related lipid peak. We acquired 154 lipid-related ions at  $m/z$  670-1000 in each HepG2 cell. 150-250 individual HepG2 cells are detected in each group.

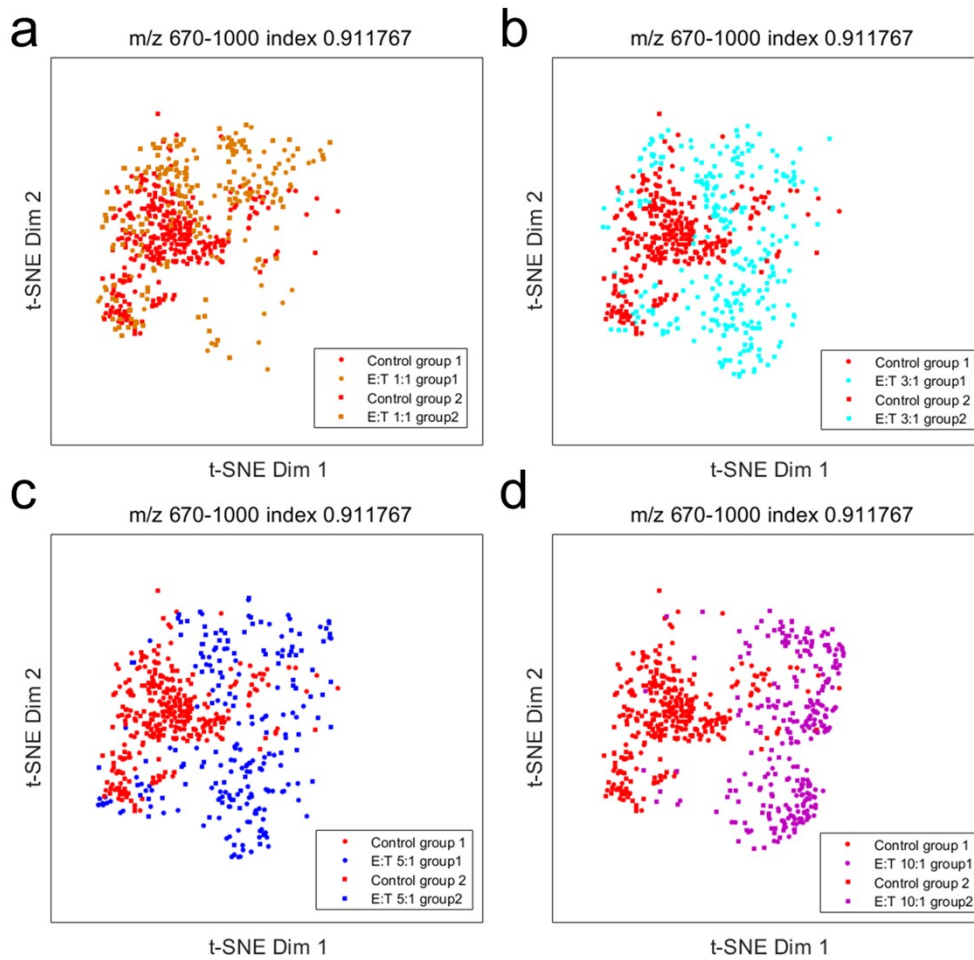


**Figure S3.** The scatter plot of individual HepG2 cells co-cultured with different amount of NK92 MI cells from E:T 1:1 to 10:1.

(a) the differences between control group and E:T 1:1. (b) the differences between control group and E:T 3:1. (c) the differences between control group and E:T 5:1. (d) the differences between control group and E:T 10:1. With the increase in the effector-target ratio (E:T), the lipid fingerprints of HepG2 cells showed increasingly difference from the control group.

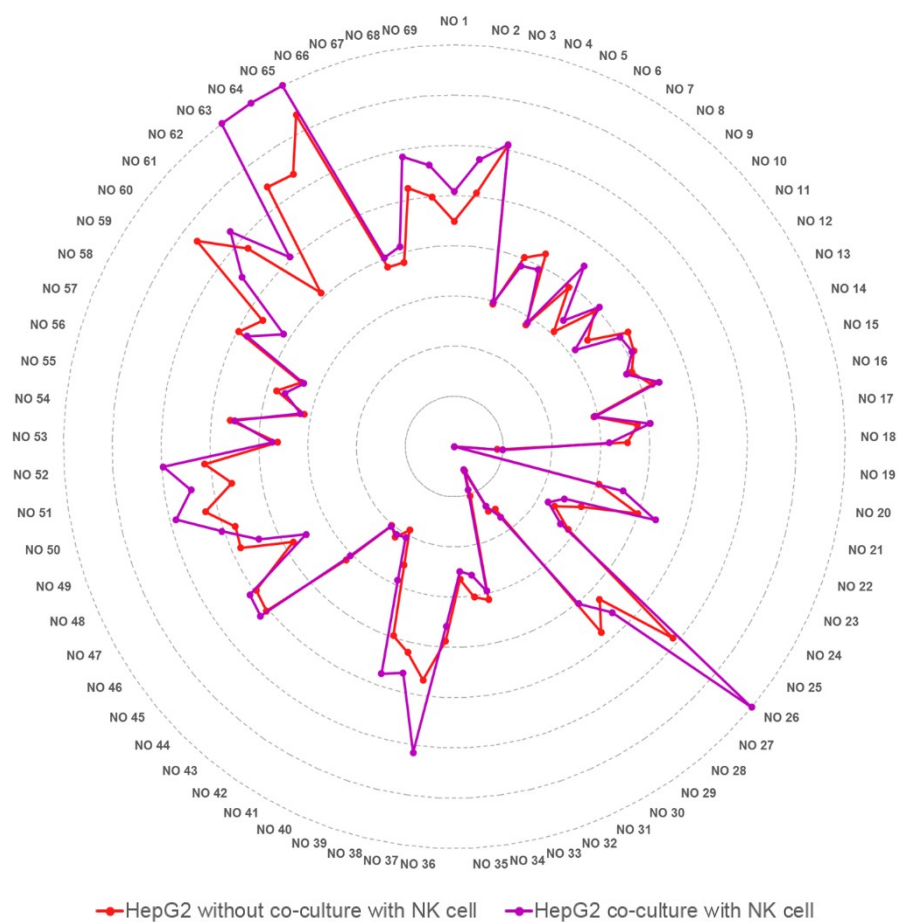


**Figure S4.** The logarithmic radar charts of average relative intensities of 69 lipids and oxidized lipids.

Lipids and oxidized lipids are sorted in ascending order of  $m/z$ . The name of lipids can be check in Table S1.

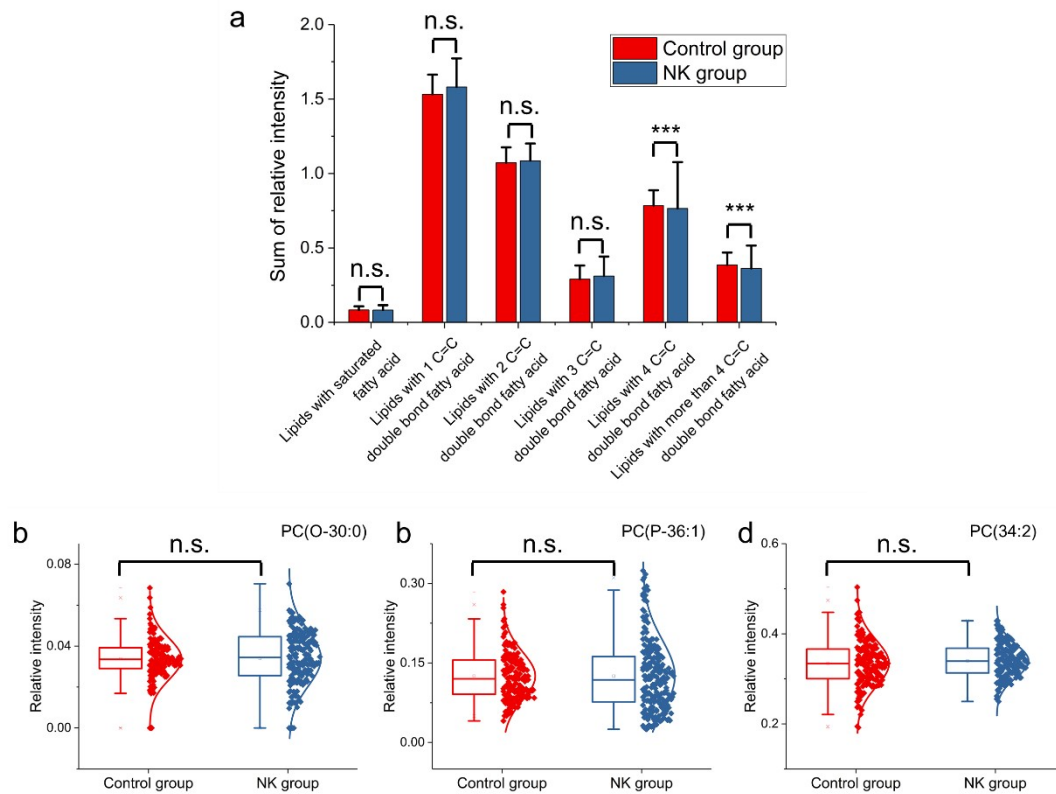


**Figure S5.** The relative intensities of different lipids between control group and NK group.

(a) The sum of relative intensities of different types of lipids between two groups. The total concentration of the two types of lipids decreased with significant difference between control group and NK group, which indicated that the part of polyunsaturated lipids were more likely to be oxidized during the NK cell-mediated apoptosis. The concentration of (b) PC(O-30:0) (c) PC(P-36:1) and (d) PC(34:2) in individual cells before and after co-culture with NK cell. There were no significant differences between two groups, which indicated that NK cell-mediated apoptosis might have little effect on these of lipids (n.s. no significant difference).

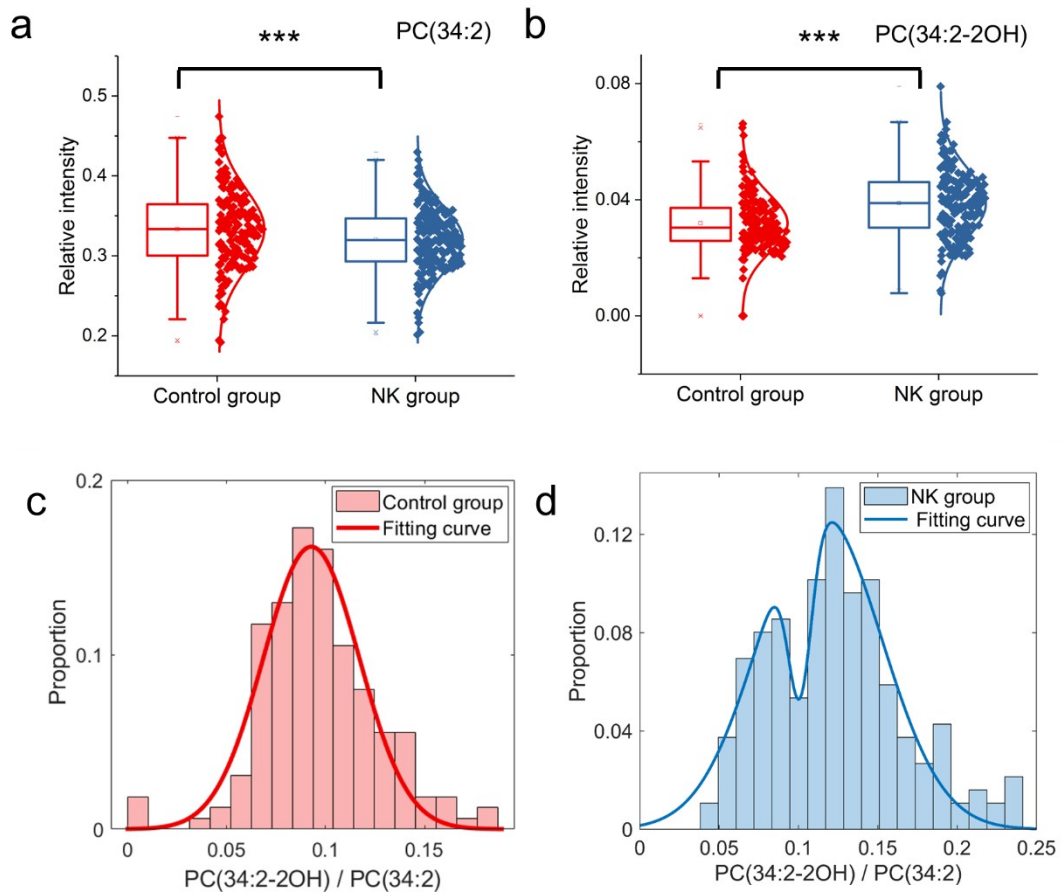


**Figure S6.** The changes of oxidized lipids in individual HepG2 cells after co-culturing with NK cells.

The concentration of (a) PC(34:2) (b) PC(34:2-2OH) in individual cells before and after co-culturing with NK cell. The concentration of PC(34:2-2OH) was increased after co-culture with NK cells, while the concentration of PC(34:2) was decreased. (c) In control group, the distribution of ratio of PC(34:2-2OH) / PC(34:2) in individual cells could be fit in a one peak Gaussian function.(d) After co-culture with NK cells, the distribution of ratio of PC(34:2-2OH) / PC(34:2) in individual cells changed from one peak to two peaks. The p-value indicated the significant differences (\*\*\*) p<0.0005).

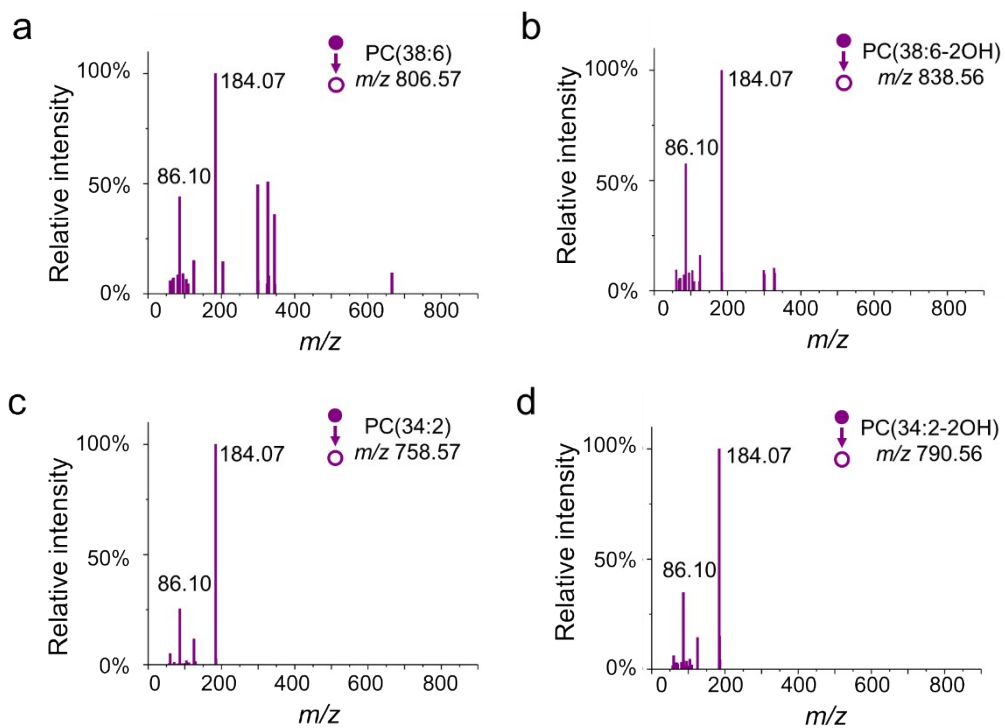


**Figure S7.** The MS<sup>2</sup> of PC(38:6), PC(38:6-2OH), PC(34:2) and PC(34:2-2OH).

The  $m/z$  184.07 is the characteristic peak of PC. The hcd is 40. (a) The MS<sup>2</sup> of PC(38:6) (b) The MS<sup>2</sup> of PC(38:6-2OH) (c) The MS<sup>2</sup> of PC(34:2) (d) The MS<sup>2</sup> of PC(34:2-2OH).

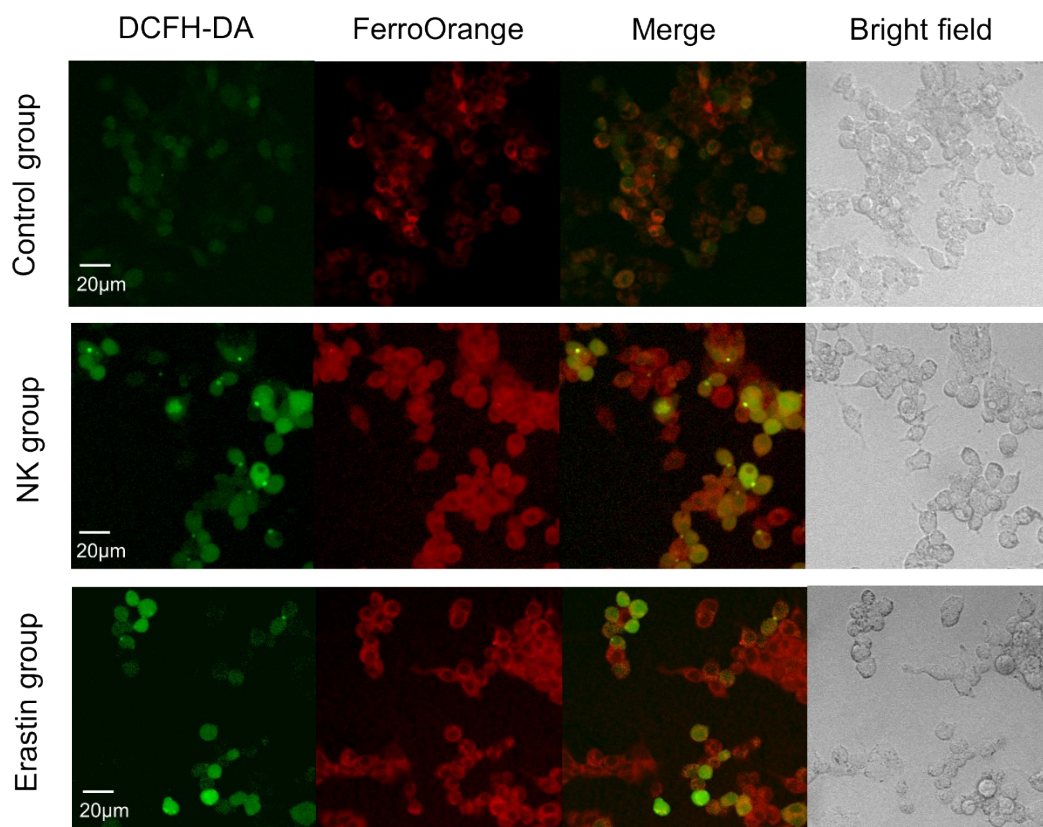


**Figure S8.** The changes of ROS and  $\text{Fe}^{2+}$  in NK group and erastin group.

The ROS was detected by DCFH-DA (green) and  $\text{Fe}^{2+}$  by FerroOrange (red). In both two groups, the concentration of  $\text{Fe}^{2+}$  and ROS increased, which indicated the above two processes were similar.

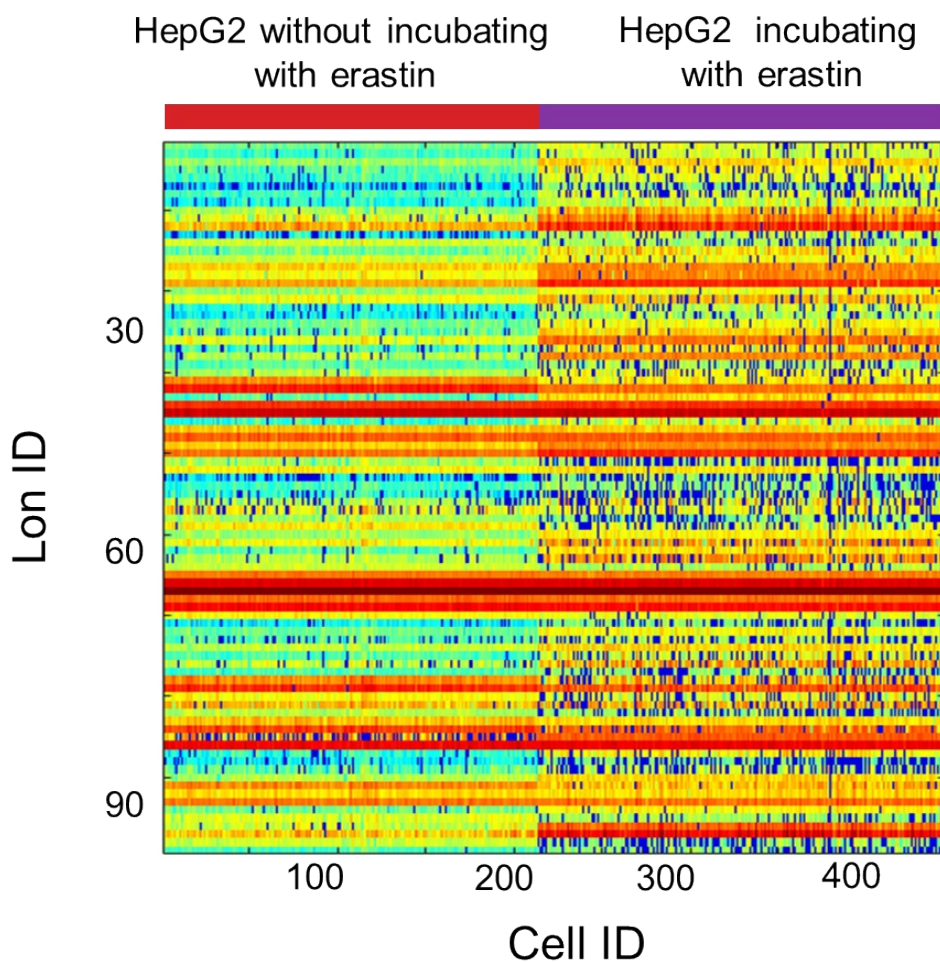


**Figure S9.** The heat map of individual HepG2 cells with and without incubating with erastin.

213 and 234 individual HepG2 cells were detected in each group. Each column of the heat map represented an individual cell and each row represented a cell-related lipid peak. We acquired 90 lipid-related ions at  $m/z$  670-1000 in each HepG2 cell.

**Table S1.** 69 lipids annotated by accurate  $m/z$ .

The lipids and oxidized lipids were annotated by accurate  $m/z$  in the positive ion mode (scan range  $m/z$  100-1000). The difference between the accurate mass of lipids and the standards mass of  $(M+H)^+$  of the lipids in database was less than 5 ppm. Since there are many isomers of lipids and lipid oxides, only one of the lipids is listed for ease of discussion.

No.	Observed mass, $m/z$	Compound name	HMDB number	Formula	Adduct	Theoretical mass, $m/z$	Error, ppm
1	674.5107	PE(P-32:1)	HMDB0011434	C <sub>37</sub> H <sub>72</sub> NO <sub>7</sub> P	M+H	674.5119	1.78
2	689.5595	SM(d33:1)	HMDB0240617	C <sub>38</sub> H <sub>77</sub> N <sub>2</sub> O <sub>6</sub> P	M+H	689.5592	0.44
3	691.4167	PA(12:0/PGE1)	HMDB0262838	C <sub>35</sub> H <sub>63</sub> O <sub>11</sub> P	M+H	691.4181	2.02
4	692.5607	PC(O-30:0)	HMDB0013341	C <sub>38</sub> H <sub>78</sub> NO <sub>7</sub> P	M+H	692.5589	2.60
5	693.5630	DG(i-39:3-2OH)	HMDB0299850	C <sub>42</sub> H <sub>76</sub> O <sub>7</sub>	M+H	693.5664	4.90
6	700.5261	PE(P-34:2)	HMDB0011343	C <sub>39</sub> H <sub>74</sub> NO <sub>7</sub> P	M+H	700.5276	2.14
7	702.5428	PE(P-34:1)	HMDB0011437	C <sub>39</sub> H <sub>76</sub> NO <sub>7</sub> P	M+H	702.5432	0.57
8	722.5090	PE(P-36:5)	HMDB0011445	C <sub>41</sub> H <sub>72</sub> NO <sub>7</sub> P	M+H	722.5119	4.01
9	724.5257	PE(P-36:4)	HMDB0011352	C <sub>41</sub> H <sub>74</sub> NO <sub>7</sub> P	M+H	724.5276	2.62
10	726.5433	PE(P-36:3)	HMDB0011442	C <sub>41</sub> H <sub>76</sub> NO <sub>7</sub> P	M+H	726.5432	0.14
11	728.5619	PE(P-36:2)	HMDB0011441	C <sub>41</sub> H <sub>78</sub> NO <sub>7</sub> P	M+H	728.5589	4.12
12	730.5774	PE(P-36:1)	HMDB0011439	C <sub>41</sub> H <sub>80</sub> NO <sub>7</sub> P	M+H	730.5745	3.97
13	731.6035	SM(d36:1)	HMDB0001348	C <sub>41</sub> H <sub>83</sub> N <sub>2</sub> O <sub>6</sub> P	M+H	731.6062	3.67
14	743.5787	DG(i-43:6-2OH)	HMDB0300349	C <sub>46</sub> H <sub>78</sub> O <sub>7</sub>	M+H	743.5820	4.44
15	749.5293	PG(34:1)	HMDB0010630	C <sub>40</sub> H <sub>77</sub> O <sub>10</sub> P	M+H	749.5327	4.67
16	750.5403	PE(P-38:5)	HMDB0011451	C <sub>43</sub> H <sub>76</sub> NO <sub>7</sub> P	M+H	750.5432	3.86
17	751.5465	PG(34:0)	HMDB0116640	C <sub>40</sub> H <sub>79</sub> O <sub>10</sub> P	M+H	751.5484	2.53
18	752.5581	PE(P-38:4)	HMDB0009412	C <sub>43</sub> H <sub>74</sub> NO <sub>7</sub> P	M+H	752.5589	1.06
19	758.5672	PC(34:2)	HMDB0008133	C <sub>42</sub> H <sub>80</sub> NO <sub>8</sub> P	M+H	758.5694	2.90
20	760.5831	PC(34:1)	HMDB0008100	C <sub>42</sub> H <sub>82</sub> NO <sub>8</sub> P	M+H	760.5851	2.63
21	766.5723	PC(P-36:4)	HMDB0011220	C <sub>44</sub> H <sub>80</sub> NO <sub>7</sub> P	M+H	766.5745	2.87
22	767.5710	SM(d38:5-OH)	HMDB0290515	C <sub>43</sub> H <sub>79</sub> N <sub>2</sub> O <sub>7</sub> P	M+H	767.5698	1.56
23	768.5932	PC(P-36:3)	HMDB0011310	C <sub>44</sub> H <sub>82</sub> NO <sub>7</sub> P	M+H	768.5902	3.90
24	770.6085	PC(P-36:2)	HMDB0011244	C <sub>44</sub> H <sub>84</sub> NO <sub>7</sub> P	M+H	770.6058	3.50
25	772.6247	PC(P-36:1)	HMDB0011307	C <sub>44</sub> H <sub>86</sub> NO <sub>7</sub> P	M+H	772.6215	4.14
26	774.6370	PC(P-36:0)	HMDB0008061	C <sub>44</sub> H <sub>88</sub> NO <sub>7</sub> P	M+H	774.6371	0.13
27	776.5560	PE(P-40:6)	HMDB0011458	C <sub>45</sub> H <sub>78</sub> NO <sub>7</sub> P	M+H	776.5589	3.73
28	778.5732	PE(P-40:5)	HMDB0009612	C <sub>45</sub> H <sub>80</sub> NO <sub>7</sub> P	M+H	778.5745	1.67
29	782.5657	PC(36:4)	HMDB0008623	C <sub>44</sub> H <sub>80</sub> NO <sub>8</sub> P	M+H	782.5694	4.73

No.	Observed mass, $m/z$	Compound name	HMDB number	Formula	Adduct	Theoretical mass, $m/z$	Error, ppm
30	784.5822	PC(36:3)	HMDB0008137	C <sub>44</sub> H <sub>82</sub> NO <sub>8</sub> P	M+H	784.5851	3.70
31	786.5989	PC(36:2)	HMDB0008039	C <sub>44</sub> H <sub>84</sub> NO <sub>8</sub> P	M+H	786.6007	2.29
32	788.6136	PC(36:1)	HMDB0008102	C <sub>44</sub> H <sub>86</sub> NO <sub>8</sub> P	M+H	788.6164	3.55
33	790.5589	PC(34:2-2OH)	HMDB0286054	C <sub>42</sub> H <sub>80</sub> NO <sub>10</sub> P	M+H	790.5593	0.51
34	792.5888	PC(P-38:5)	HMDB0011319	C <sub>46</sub> H <sub>82</sub> NO <sub>7</sub> P	M+H	792.5902	1.77
35	794.6093	PC(P-38:4)	HMDB0011253	C <sub>46</sub> H <sub>84</sub> NO <sub>7</sub> P	M+H	794.6058	4.40
36	796.6208	PC(P-38:3)	HMDB0011316	C <sub>46</sub> H <sub>86</sub> NO <sub>7</sub> P	M+H	796.6215	0.88
37	800.5428	PE(38:4-2OH)	HMDB0285864	C <sub>43</sub> H <sub>78</sub> NO <sub>10</sub> P	M+H	800.5436	1.00
38	800.6122	PC(37:2)	HMDB0256163	C <sub>45</sub> H <sub>86</sub> NO <sub>8</sub> P	M+H	800.6126	0.50
39	804.5499	PC(38:7)	HMDB0008436	C <sub>46</sub> H <sub>78</sub> NO <sub>8</sub> P	M+H	804.5538	4.85
40	806.5664	PC(38:6)	HMDB0008434	C <sub>46</sub> H <sub>80</sub> NO <sub>8</sub> P	M+H	806.5694	3.72
41	808.5865	PC(38:5)	HMDB0008433	C <sub>46</sub> H <sub>82</sub> NO <sub>8</sub> P	M+H	808.5851	1.73
42	810.5975	PC(38:4)	HMDB0008331	C <sub>46</sub> H <sub>84</sub> NO <sub>8</sub> P	M+H	810.6007	3.95
43	813.6831	SM(d42:2)	HMDB0240635	C <sub>47</sub> H <sub>93</sub> N <sub>2</sub> O <sub>6</sub> P	M+H	813.6844	1.60
44	815.6986	SM(d42:1)	HMDB0011697	C <sub>47</sub> H <sub>95</sub> N <sub>2</sub> O <sub>6</sub> P	M+H	815.7001	1.84
45	818.6056	PC(P-40:6)	HMDB0008721	C <sub>48</sub> H <sub>84</sub> NO <sub>7</sub> P	M+H	818.6058	0.24
46	819.6018	SM(d42:6-OH)	HMDB0290755	C <sub>47</sub> H <sub>83</sub> N <sub>2</sub> O <sub>7</sub> P	M+H	819.6011	0.85
47	820.6185	PC(P-40:5)	HMDB0011325	C <sub>48</sub> H <sub>86</sub> NO <sub>7</sub> P	M+H	820.6215	3.66
48	822.6336	PC(P-40:4)	HMDB0011259	C <sub>48</sub> H <sub>88</sub> NO <sub>7</sub> P	M+H	822.6371	4.25
49	826.5626	PE(40:5-2OH)	HMDB0284080	C <sub>45</sub> H <sub>80</sub> NO <sub>10</sub> P	M+H	826.5593	3.99
50	829.6788	SM(d42:1-OH)	HMDB0013469	C <sub>47</sub> H <sub>93</sub> N <sub>2</sub> O <sub>7</sub> P	M+H	829.6793	0.60
51	830.5691	PC(40:8)	HMDB0008443	C <sub>48</sub> H <sub>80</sub> NO <sub>8</sub> P	M+H	830.5694	0.36
52	831.5708	PG(i-39:3-OH)	HMDB0272073	C <sub>45</sub> H <sub>83</sub> O <sub>11</sub> P	M+H	831.5746	4.57
53	832.5821	PC(40:7)	HMDB0008213	C <sub>48</sub> H <sub>82</sub> NO <sub>8</sub> P	M+H	832.5851	3.60
54	833.5879	PG(i-39:1-O)	HMDB0272042	C <sub>45</sub> H <sub>85</sub> O <sub>11</sub> P	M+H	833.5902	2.76
55	834.5987	PC(40:6)	HMDB0008631	C <sub>48</sub> H <sub>84</sub> NO <sub>8</sub> P	M+H	834.6007	2.40
56	835.5999	SM(d42:7-2OH)	HMDB0290754	C <sub>47</sub> H <sub>83</sub> N <sub>2</sub> O <sub>8</sub> P	M+H	835.5960	4.67
57	836.6130	PC(40:5)	HMDB0008630	C <sub>48</sub> H <sub>86</sub> NO <sub>8</sub> P	M+H	836.6164	4.06
58	838.5555	PC(38:6-2OH)	HMDB0286590	C <sub>46</sub> H <sub>80</sub> NO <sub>10</sub> P	M+H	838.5593	4.53
59	838.6279	PC(40:4)	HMDB0008628	C <sub>48</sub> H <sub>88</sub> NO <sub>8</sub> P	M+H	838.6320	4.89
60	840.6469	PC(40:3)	HMDB0008119	C <sub>48</sub> H <sub>90</sub> NO <sub>8</sub> P	M+H	840.6477	0.95
61	842.6597	PC(40:2)	HMDB0008150	C <sub>48</sub> H <sub>92</sub> NO <sub>8</sub> P	M+H	842.6633	4.27
62	854.5712	PC(42:10)	HMDB0008739	C <sub>50</sub> H <sub>80</sub> NO <sub>8</sub> P	M+H	854.5694	2.11
63	858.5829	PC(PGD2/18:0)	HMDB0286231	C <sub>46</sub> H <sub>84</sub> NO <sub>11</sub> P	M+H	858.5855	3.03
64	869.6977	PA(48:2)	HMDB0115481	C <sub>51</sub> H <sub>97</sub> O <sub>8</sub> P	M+H	869.6994	1.95
65	870.6912	PC(42:2)	HMDB0008763	C <sub>50</sub> H <sub>96</sub> NO <sub>8</sub> P	M+H	870.6946	3.90
66	880.5889	PC(44:11)	HMDB0008746	C <sub>52</sub> H <sub>82</sub> NO <sub>8</sub> P	M+H	880.5851	4.32
67	882.6018	PC(44:10)	HMDB0008745	C <sub>52</sub> H <sub>84</sub> NO <sub>8</sub> P	M+H	882.6007	1.25
68	885.5414	PE(P-18:1/LTE4)	HMDB0285514	C <sub>46</sub> H <sub>81</sub> N <sub>2</sub> O <sub>10</sub> PS	M+H	885.5422	0.90
69	887.5598	PE(P-18:0/LTE4)	HMDB0285309	C <sub>46</sub> H <sub>83</sub> N <sub>2</sub> O <sub>10</sub> PS	M+H	887.5579	2.14